Evaluating Resonances in PCSEL Structures based on Modal Indices

Guangrui Li [1*], Jayanta Sarma [2], Richard Hogg [1]

[1] School of Engineering, University of Glasgow, Glasgow, G12 8TL, UK
[2] Visiting researcher

[*]g.li.2@research.gla.ac.uk

Abstract: The frequently sought after combination of characteristics in semiconductor lasers of high power together with narrow beam divergence and monochromatic output is usually difficult to attain. The photonic crystal surface emitting laser (PCSEL) is one category of device, however, which tends to provide the above mentioned desirable output features. The PCSEL uses a large area optically active surface but with a 2-D periodic structure that enables it to generate high power in a narrow vertically emitted beam yet maintaining single wavelength operation. A primary requirement to model PCSELs is to obtain the optical field resonances that identify the lasing mode. This paper presents an alternative method for evaluating the resonances, based essentially on the transfer-matrix technique and wave propagation in multilayer medium, which is relatively easy to formulate, and has quite modest demands on computing requirements.

1. Introduction

Lasers, particularly semiconductor lasers, with their extensive applications in nearly all aspects of modern society have become ubiquitous since the 1980s - and yet, the search continues for such devices with increasingly demanding operational characteristics. Perhaps the most frequently sought after combination of characteristics in semiconductor lasers are high power combined with narrow beam divergence and monochromatic (narrow linewidth) output[1]. As is well known, these three features are seemingly incompatible to achieve together in typical semiconductor lasers; broadly speaking, high power and narrow beam divergence require large active area but that leads to spatial multi-moding and hence multi wavelength (non-monochromatic) output. Many kinds of device structures such as coupled parallel stripe contact [2], adiabatically tapered stripe contact [3], etc. devices have been studied to achieve the above mentioned combination of desirable output characteristics with various degrees of success, but the pursuit has continued. One of the devices that has gained particular prominence in that direction in recent years is the photonic crystal surface emitting laser (PCSEL). The PCSEL consists of essentially a large optically active area which has the potential to generate large optical power while retaining low optical power density and emitting in a narrow beam. The problem, however, that a large area structure is typically prone to supporting a large number of very closely spaced resonances leading to the strong likelihood of multi-mode lasing, is counteracted in this instance by the use of a photonic crystal (PC) structured surface area.

Wave propagation in periodic media has been studied for over a century [4] but the topic has received very significant resurgence in recent years with the introduction of the concept of PCs [5]. Large volumes of research publications have subsequently appeared in the study and application of PCs in such diverse areas as PC fibres[6, 7], PC planar waveguides and resonators [8-10] and optical sources such as PCSELs[11]. Thus, several techniques for analysing (specially optical) waves in periodic media exist in the published literature, but the three, plane wave expansion (PWE) [12], coupled mode theory (CMT) [13], and the purely numerical finite difference time domain (FDTD) [14], are by far the most extensively used. The PWE method is based on representing the field in the PC by a (complete) set of plane-waves (PWs) [15], while the effect of media periodicity is enforced by a Floquet-Bloch function representation. However, note that an infinitely large medium of unvarying periodicity is implicit in this formulation (i.e., an infinite number of identical periodic layers). Consequently, with the PWE method it is not readily possible to analyse periodic media of finite extent (finite number of identical periodic layers). Such limitations are removed if the CMT is used [16], but the mathematical complexities involved are somewhat daunting for the average user and requires very considerable effort and time to implement. The FDTD is a purely numerical method and may be used to solve for fields in almost any kind of structure [17]; typically, however, considerable computer resources are needed and significantly long computation times are required [18]. In view of the above, there is a noticeable need to develop another technique to solve for fields in 2-d PCs – pertinent to PCSELs - which is relatively simple, easy to implement and requires modest resources and time while retaining a 'physical feel'.

A primary requirement to model PCSELs is to obtain the optical field resonances that identify the lasing mode. This paper presents an alternative method for evaluating the resonances, based essentially on the transfer-matrix technique and wave propagation in multilayer medium, which is relatively easy to formulate, and has quite modest demands on computing requirements. Such a technique, particularly suited to rectangular geometry structures, has been developed and is described in this paper. It is envisaged that the implementation of this method will enhance the potential to generate more comprehensive models of photonic crystal based devices, say, PCSELs, that include, for example, aspects of inversion-population distribution and also time dependence while still retaining relatively modest demands on computational resources.

2. Description of model

As stated above, the objective is to develop a modelling technique that is easy to implement and use but which reliably yields the essential quantitative characteristics of PC structures, particularly relevant to PCSELs. A rectangular co-ordinate system (x, y, z) consistent with the rectangular device geometry is used throughout. Thus refer to Fig. [1] which gives a schematic representation of a planar periodic structure in the *x*-z plane defined by rectangular regions of widths w_a , w_b and refractive index, η_a surrounded by regions with refractive index η_b ; the periodicities of the structure are L_a , L_b . Although not essential to this method, for the purposes of this paper the relative magnetic permeability $\mu = 1$, is assumed throughout, as is the case for most semiconductor material for optical devices, so that the relative electrical permittivity, $\varepsilon = \eta^2$ is applicable.

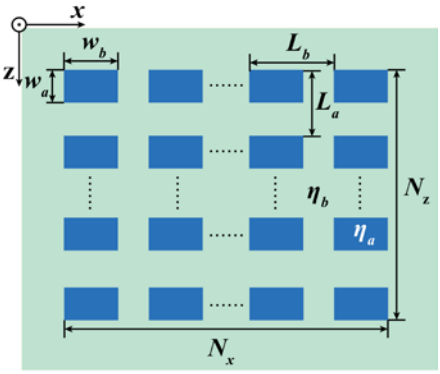

Fig. 1 Schematic of PC structure. N_x and N_z are number of periods along *x* and z respectively.

This refractive index pattern $\eta(x, z)$ may be produced by actual, direct material growth and/or by some post growth fabrication process. For example, appropriate variation in the material composition of the vertical layers and/or thicknesses (y axis) is often used to produce a variation in the vertical guided mode that may then be considered as creating an effective-index pattern $\eta(x, z)$ in the *x*-z plane [18] corresponding to that in Fig.[1]. However, henceforth in this paper the study is restricted to a 2-D analysis (in the *x*-z plane); i.e., essentially $\eta(x, y, z) = \eta(x, z)$ and the excitation is such that any non-zero field component, $\hat{F}(x, y, z) = \hat{F}(x, z)$ [18], i.e., $\partial/\partial y \approx 0$ is applicable; then, approximately, two independent categories of field solutions, one with polarisation , $TE_y \Rightarrow E_y = 0$ and the other with $TM_y \Rightarrow H_y = 0$ can be sustained [16, 19]. To be specific, $\hat{F}(x, z)$ will be used to represent the non-zero y-directed field component. For application to PCSELs the TE_y polarisation is important since the typical active-layer gain medium supports this polarisation; thus, H_y, E_x, E_z are the dominant non-zero field components in that case.

In a region with $\varepsilon(x, z) = \eta^2(x, z)$ and for harmonic time dependent $\exp(j\omega t)$ fields, the application of Maxwell's equations and following the commonly accepted assumption $\mathbf{E} \cdot \nabla\varepsilon \sim 0$ leads to the wave equation

$$\left[\frac{\partial^2}{\partial x^2} + \frac{\partial^2}{\partial z^2} + k_0^2 \eta^2(x, z)\right] \hat{F}(x, z) = 0 \qquad (1)$$

where $k_0^2 = (2\pi/\lambda_0)^2 = \omega^2 \mu_0 \varepsilon_0$. The 2-D PC structure that is considered in this paper is shown in Fig. [1] where piece-wise constant, rectangular regions are assumed with abrupt transitions between regions with $\eta = \eta_a$ and $\eta = \eta_b$; this represents $\eta(x, z)$ in eqn.(1). The field distribution $\hat{F}(x, z)$ for the resonant modes $(m, n;$ integers) of this PC structure are considered to be of the form

$$\hat{F}_{m,n}(x, z) = f_m(x) g_{n,m}\left[z; f_m(x)\right] \qquad (2)$$

corresponding to the resonant wavelength $\lambda_{0\,m,n}$. The notation $g_{n,m}\left[z; f_m(x)\right]$ simply emphasises the point that the solution $g_{n,m}$ depends on the solution f_m, which becomes clear in the detailed discussion below. Note that $\hat{F}_{m,n}(x, z)$ is, in general, a non-separable function but in the context of present typical device parameters such as dimensions, magnitudes of refractive index discontinuities, etc., it is justifiably acceptable to assume a separated variable form for each resonant mode of the 2D-PC.

The essential underlying concept of the analysis procedure presented here is based on viewing the 2D-PC structure of Fig. [1] as a laterally (say, along *x*) multilayer waveguide which is longitudinally (along z) segmented. Hence the required 2D field distributions are evaluated as modes propagating in multilayer waveguides with longitudinal discontinuities. Analysing waveguide discontinuities is quite complicated [20] since, in general, each incident mode excites all the other modes. However, in the present context of dimensions and magnitude of discontinuities etc. it is justified to assume that only the same (single) mode as that incident exists throughout and this simplification will apply to the analysis that is used here to solve for the 2D-PC resonances

Thus, the procedure for obtaining $\hat{F}_{m,n}(x, z)$, $\lambda_{0\,m,n}$ begins by first evaluating the modes of the longitudinally uniform (i.e., *not* segmented) multilayer waveguide, structure as shown in Fig. [2a] with $\eta = \eta_x(x)$ corresponding to the pattern defined by Fig. [1]. The wave equation for the structure in Fig. [2a] is then

$$\left[\frac{\partial^2}{\partial x^2} + \frac{\partial^2}{\partial z^2} + k_0^2 \eta_x^2(x)\right] F(x, z) = 0 \qquad (3)$$

Clearly, a separation of variables solution is applicable with eigen-mode/eigen-value solutions (f_m , β_m) , similar to those for multilayer slab dielectric waveguides

$$F(x, z) = f_m(x) e^{-j\beta_m z} \qquad (4)$$

satisfies eqn.(3). Full use is made of piecewise constant slab dielectric regions to generate a transfer matrix formulation, denoted $\mathbf{M}_T$, to numerically solve [21] for $f_m(x)$ and β_m .

Rather than solve for the modes in the periodic multilayer waveguide structure, Fig.[2a], directly as an eigenvalue problem, it is found to be more convenient and illustrative to treat it as an excitation problem. It is known that the eigen-mode of the finite 1-D periodic structure can be represented by the total transmittance solution of such a structure [22]. As shown in Fig.[2a] a plane wave (PW)

incident at an angle θ excites corresponding PWs in the multilayer regions, η_a , η_b such that $\kappa_a^2+\beta^2=k_0^2\eta_a^2$ and $\kappa_b^2+\beta^2=k_0^2\eta_b^2$ where κ and β represent the *x*-directed and z-directed propagation constants in the corresponding regions. Applying the usual field matching conditions at the abrupt interfaces [23] between regions 'a' and 'b' yields the elements of the 2 x 2 unimodular transfer matrix, **m**, for a typical unit cell[24].

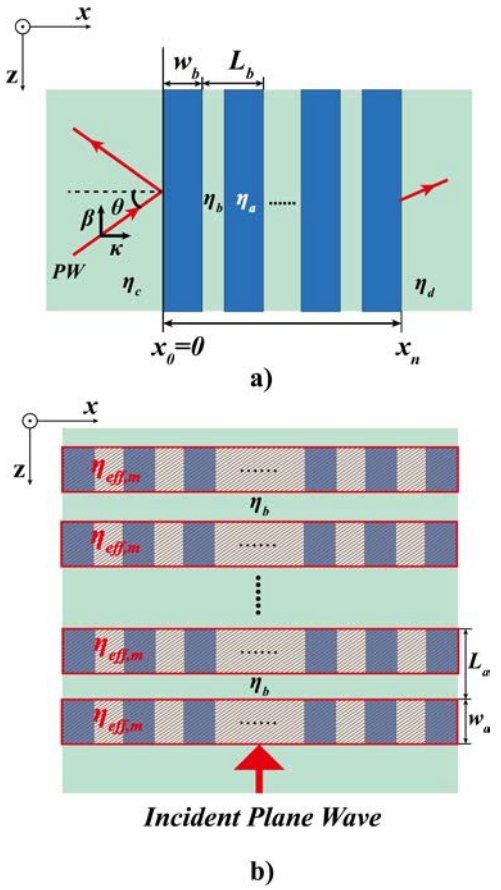

Fig. 2 Model description: (Refractive indices: η_a , $\eta_b=\eta_c=\eta_d$) **a)** Lateral modes propagating along the z-axis are computed for a relevant range of wavelengths. **b)** The shaded area with dark blue region representing the multilayer waveguide in Fig. 2a) is replaced by a homogeneous medium of effective modal index $\eta_{eff,\,m}$, thus resulting in a 1-D periodic grating along z with an unit cell composited of $\eta_{eff,\,m}$ and η_b

Further, and very importantly, the periodic nature of the multilayer medium is utilised to obtain a compact and very efficient formulation for the composite transfer matrix accounting for the corresponding number, N , of periodic layers [25]. Thus the total transfer matrix is given by $\mathbf{M}_T=\mathbf{m}^N$ where **m** is the unimodular transfer matrix in a unit cell:

$$\mathbf{M}_T=\mathbf{m}^N=\begin{pmatrix} m_{11} & m_{12} \\ m_{21} & m_{22}\end{pmatrix}^N = \begin{pmatrix} m_{11}U_{N-1}-U_{N-2} & m_{12}U_{N-1} \\ m_{21}U_{N-1} & m_{22}U_{N-1}-U_{N-2}\end{pmatrix} \quad (5)$$

m_{11} , m_{12} , m_{21} and m_{22} are the matrix elements, and U_N are known as Chebyshev polynomials of the second kind (see Appendix):

$$U_N=\frac{\sin\left[(N+1)\cos^{-1}\left(\frac{m_{11}+m_{22}}{2}\right)\right]}{\sin\left[\cos^{-1}\left(\frac{m_{11}+m_{22}}{2}\right)\right]} \quad (6)$$

There are many different methods to calculate power N of unimodular 2×2 matrix [22, 26] which enables analysing a truncated periodic structure since, unlike infinite periodic structures, the Bloch theorem does not strictly apply in this situation [20][27]. This procedure is also beneficial since it provides for a significantly reduced computation time. The resonant mode for the entire multilayer (periodic) structure can be calculated from the total transfer matrix, which effectively is the solution of a transcendental equation: $\left|m_{11}U_{N-1}-U_{N-2}\right|=1$ [25].

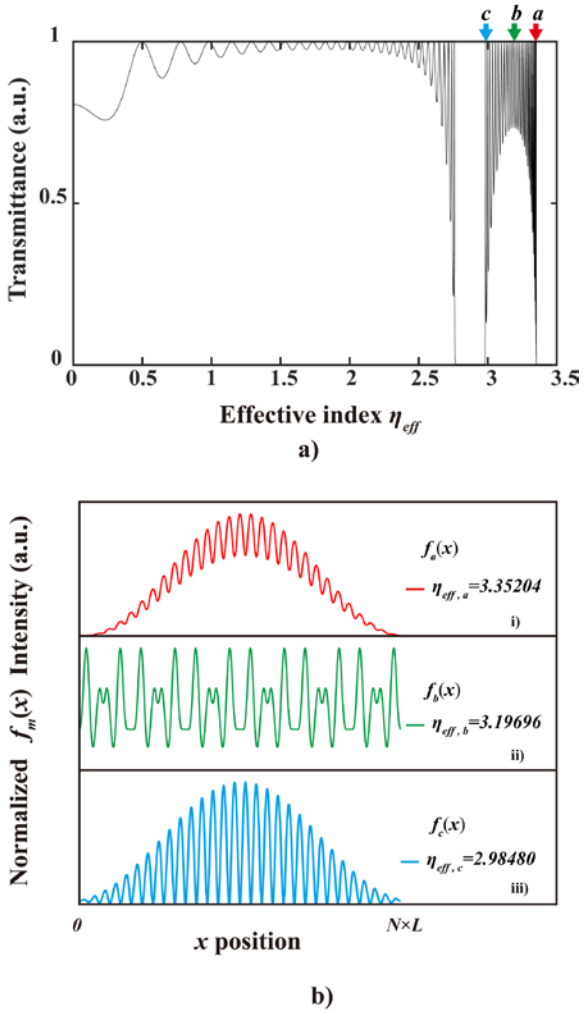

Fig. 3 a) Transmission spectrum of periodic structure (referring to Fig. 2a, $N=30$, $L_b=286.25nm$, $w_b=116.5nm$, $\eta_a=3.13$, $\eta_b=3.46$.)

b) Examples of eigen-mode solutions $f_m(x)$ of 1-D periodic structure (Fig 2a)

For a relevant range of wavelengths, transmission resonances for plane waves incident on the multilayer input at $x=0$,at incident angles, $0<\theta<\pi/2$, are used to identify the eigen-mode solutions [28]; the incident angles

corresponding to transmission resonances provide the β_m and corresponding $f_m(x)$. An example of power transmittance through the 1-D periodic structure, Fig.[2a], with $N_x = N = 30$ is shown in Fig.[3a]; points a, b and c are given as examples of eigen mode solutions which corresponds to 1-D transmission resonances. The corresponding typical field distributions labelled as $f_m(x)$ $(m = a,b,c)$ are shown in Fig.[3b].

The modal propagation constant $\beta_m = k_0 \eta_{eff,\,m}$ is often referred to as the modal effective index $\eta_{eff,\,m}$ and also gives the mode impedance; that is, for the next stage of the analysis, the composite multilayer structure along *x*-axis supporting mode $f_m(x)$ can be replaced by $\eta_{eff,\,m}$ (or by the corresponding modal impedance).

The second stage of the analysis proceeds by now incorporating the discontinuities along the z-axis of the multilayer waveguide. This is done by representing the length along z of the multilayer waveguide region by the corresponding mode index, $\eta_{eff,\,m}$, followed by the length of the discontinuity, gap region of index η_b . This results in the 1-D multilayer structure (periodic grating) as shown in Fig. [2b]. It is worth reminding that the above representation follows from the previously stated justifiable approximation of a separated variables solution for the resonant modes of the 2D-PC; this follows from accepting that each waveguide mode, $f_m(x)$, excites only the same single mode even at the waveguide discontinuities.

The resonances for this 1-D grating are now sought, over the same wavelength range as before, by considering the response to a perpendicularly incident plane wave; the transfer matrix method, as described previously with reference to Fig. [2a] is used also here to obtain the result. Thus, with reference to Fig. [2b] the field distribution along z at resonance, $g_{n,m}\left[z; f_m(x)\right]$, is obtained and the final result, in effect, includes reasonably well the characteristics of the original 2-D periodic media (Fig. [1]). Hence the final 2-D field distributions at resonances, $\lambda_{0\,m,n}$, are $\hat{F}_{m,n}(x,z) = f_m(x) g_{n,m}\left[z; f_m(x)\right]$.

The very important point to note is that this scheme for determining 2-D PC resonances is computationally extremely fast so that results for even a very fine subdivision of wavelengths and for 2-D structures with very large N (~10^6) can be generated in tens of minutes in a simple desktop computer. Hence a very detailed search of possible 2-D resonances becomes readily possible. Note, interestingly that there can be regions of wavelengths for which 2-D resonances do not occur even though many corresponding x-directed modes $\left[f_m(x), \beta_m\right]$ exist; this region of wavelengths correspond to stop-bands in periodic structures.

3. Results and discussions

The mode index analysis (MIA) modelling method described above is applied to obtain numerical results for 2-D PC structures, Fig. [1], with $L_a = L_b = L$, $w_a = w_b = w$ and $N_x = N_z = N$ chosen for convenient comparison with results presented by other researchers (e.g., [29], [30]).

Fig. [4a] shows the (final) TE_y resonances of a finite 2-D periodic structure with $N = 250$, $\eta_a = 3.13$, $\eta_b = 3.46$, $L = 286.25nm$, $w = 116.5nm$ within the wavelength range, $0.8\mu m < \lambda_0 < 1.2\mu m$; these values correspond to those used in [29].

For each λ_0 the modes $f_m(x)$ for the periodic waveguide structure, Fig. [2a], are obtained and the corresponding $\eta_{eff,m}$ are represented along one axis in Fig. [4a]. Of these, the ones that also show unity transmission along z, Fig.[2b], are shown as red dots in Fig.[4a] and correspond to the sought resonances of the 2D PC, Fig.[1].

When N~10^6 is used, (i.e. , $N \to \infty$) , with the MIA method the wavelengths corresponding to the two points marked Mode 1 and Mode 2 in Fig.[4a] match very closely with the wavelengths corresponding to the band edge Mode 1 and Mode 2 in Fig. [4b] which were computed using the PWE method for a 2-D PC structure with dimensions and refractive indices identical to that used to obtain the results in Fig. [4a]. This demonstrates that the MIA method presented above yields reliable results.

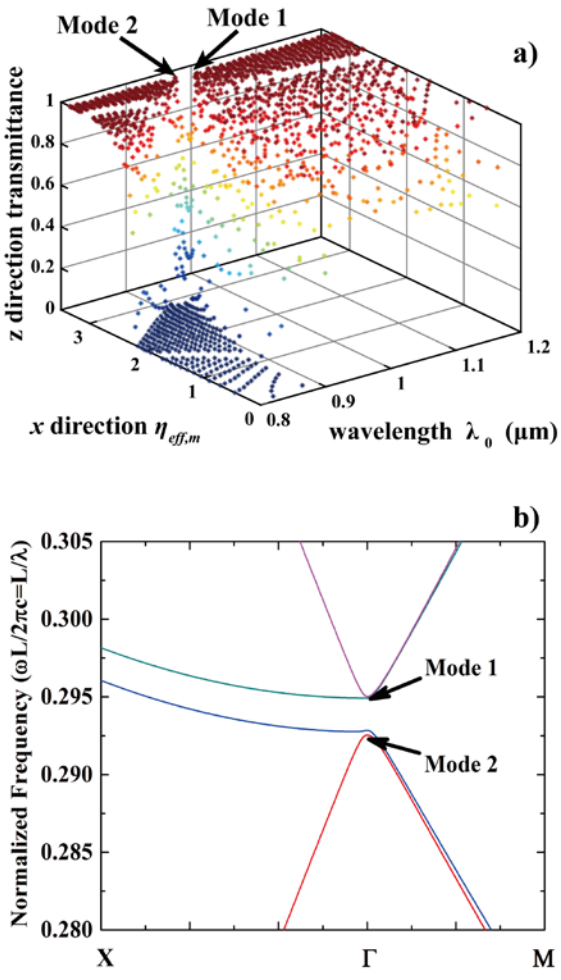

Fig. 4 a) 2-D resonances of PC calculated using MIA. (Band edge resonances: Mode 1 and Mode 2) **b)** Photonic band structure calculated using PWE. (Band edge resonances: Mode 1 and Mode 2)

Further evidence of the validity of this new MIA method is seen from Fig [5a] which shows the variation of the band edge resonance of TE_y polarization with the change in the filling-factor, w^2/L^2 [11]. Again, N~ 10^6 has been chosen in the MIA for compatible comparisons with the PWE results. The red dots and blue triangles are two band edge modes calculated using PWE, the black circles and green triangles are the corresponding modes calculated using MIA. It can be seen that the results from the two methods match extremely well over a very large range of filling-factors. This provides further proof that the MIA method yields very reliable results.

The finite size effect on the 2-D resonance of PCs has also been observed by this model. Shown in Fig.[5b], are the results for Mode 1 and Mode 2 (refer Figs. [4a, 4b]) but now with a smaller N range of $20 \rightarrow 1000$. The dots and triangles are results from MIA while the dashed lines are results using the PWE method. Note that for N < 150 the MIA results deviate from the PWE since the latter method is valid for $N \rightarrow \infty$ .This illustrates the wide range of applicability of the MIA method and so it can be used, e.g., to better identify the lasing wavelength in PCSELs when N is small.

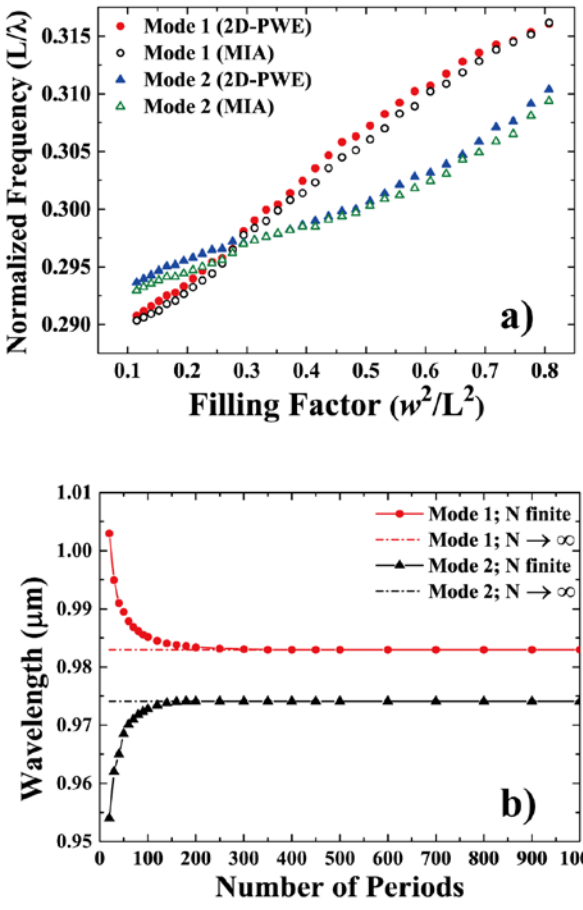

Fig. 5 a) Band edge resonances calculated with varying filling factor. **b)** Finite size effect on band edge resonance.

Fig. [6a] is a MIA generated plot of $\left|\hat{F}(x,z)\right|$ for the band-edge mode of a 2-D PC structure. The size of the PC region used in modelling is $70\mu m \times 70\mu m$ with $L = 286.25nm$, $w = 116.5nm$. This single lobed field distribution corresponding to the lasing mode matches well with that obtained by CMT[30]. A detail of the plot of $\left|\hat{F}(x,z)\right|$ at the centre of the lobe using MIA is shown in Fig. [6b] and using PWE in Fig. [6c]. It is seen that the plots match very favourably.

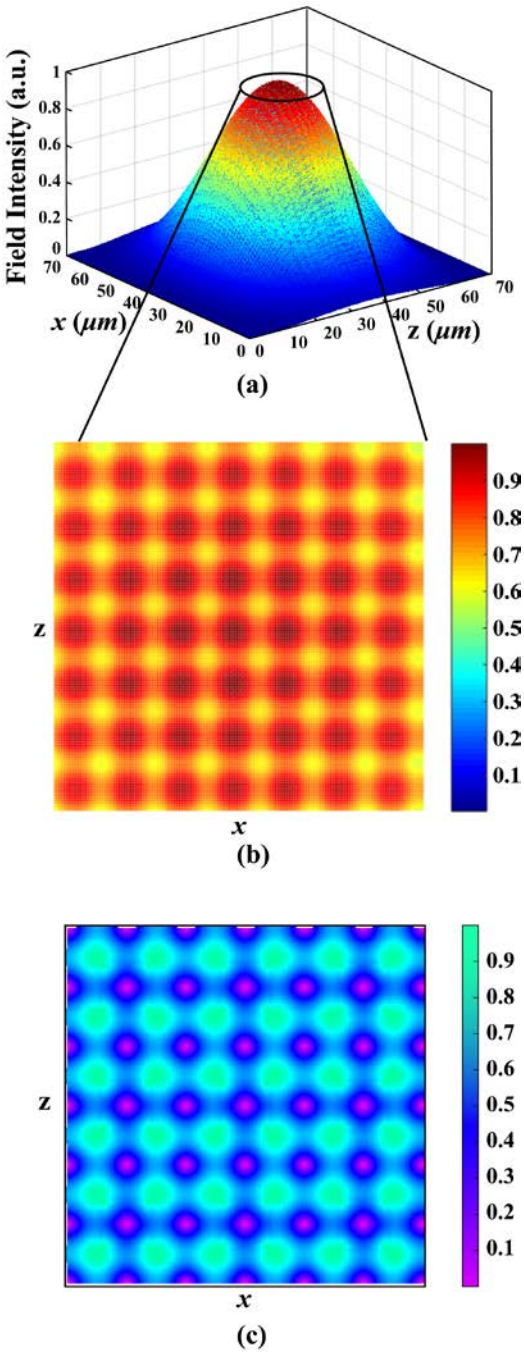

Fig. 6 a) Plot of field distribution $\left|\hat{F}(x,z)\right|$ for band-edge mode. ($N_x = N_z = 250$)**b)** A detail of the plot of $\left|\hat{F}(x,z)\right|$ at the centre of the lobe using MIA**. c)** A detail plot of $\left|\hat{F}(x,z)\right|$ using PWE by assuming infinite number of periods ($N \rightarrow \infty$).

4. Conclusions

This paper presents a novel, mode index analysis (MIA) method for solving the modes and resonances of 2-D

PCs. The properties of wave propagation in multilayer periodic medium and transverse resonance concepts are utilised to generate a computational process that is quasi-analytic and hence considerably fast. The MIA is easy to implement and is shown here by comparisons with results from other well-established methods to yield very acceptable results for rectangular geometry structures. Several numerical experiments have been carried out to demonstrate the validity of the MIA model. In view of its convenience and speed of operation the MIA method is being developed further to enable more comprehensive modelling of active devices such as PCSELs to include, for example, spatial and temporal variation in optical gain and other PC configurations. The MIA method has the potential to be extended to also analyse periodic structures with defects [31] and quasi-periodic structures [32]; the possible schemes to achieve these objectives are being considered for continued investigations.

5. Acknowledgements:

The authors wish to thank the referees for their insightful and informative comments which have been helpful and useful.

6. References

[1] L. A. Coldren, S. W. Corzine, and M. L. Mashanovitch, *Diode lasers and photonic integrated circuits*. John Wiley & Sons, 2012.

[2] D. Botez, "Monolithic phase-locked semiconductor laser arrays," *Diode Laser Arrays*, 1994.

[3] F. Causa and J. Sarma, "Realistic model for the output beam profile of stripe and tapered superluminescent light-emitting diodes," *Applied optics*, vol. 42, no. 21, pp. 4341-4348, 2003.

[4] L. Brillouin, *Wave propagation in periodic structures: electric filters and crystal lattices*. Courier Corporation, 2003.

[5] E. Yablonovitch, "Inhibited spontaneous emission in solid-state physics and electronics," *Physical review letters*, vol. 58, no. 20, p. 2059, 1987.

[6] P. Russell, "Photonic crystal fibers," *science*, vol. 299, no. 5605, pp. 358-362, 2003.

[7] T. A. Birks, J. C. Knight, and P. S. J. Russell, "Endlessly single-mode photonic crystal fiber," *Optics letters*, vol. 22, no. 13, pp. 961-963, 1997.

[8] D. Usanov and A. Skripal, "Photonic Crystal Waveguides," in *Emerging Waveguide Technology*: IntechOpen, 2018.

[9] A. Mekis, J. Chen, I. Kurland, S. Fan, P. R. Villeneuve, and J. Joannopoulos, "High transmission through sharp bends in photonic crystal waveguides," *Physical Review Letters*, vol. 77, no. 18, p. 3787, 1996.

[10] T. F. Krauss, "Slow light in photonic crystal waveguides," *Journal of Physics D: Applied Physics*, vol. 40, no. 9, p. 2666, 2007.

[11] M. Meier *et al.*, "Laser action from two-dimensional distributed feedback in photonic crystals," *Applied Physics Letters*, vol. 74, no. 1, pp. 7-9, 1999.

[12] M. Plihal and A. Maradudin, "Photonic band structure of two-dimensional systems: The triangular lattice," *Physical Review B*, vol. 44, no. 16, p. 8565, 1991.

[13] I. Vurgaftman and J. R. Meyer, "Design optimization for high-brightness surface-emitting photonic-crystal distributed-feedback lasers," *IEEE Journal of Quantum electronics*, vol. 39, no. 6, pp. 689-700, 2003.

[14] S. Fan and J. Joannopoulos, "Analysis of guided resonances in photonic crystal slabs," *Physical Review B*, vol. 65, no. 23, p. 235112, 2002.

[15] K. Leung and Y. Liu, "Photon band structures: The plane-wave method," *Physical Review B*, vol. 41, no. 14, p. 10188, 1990.

[16] M. Toda, "Proposed cross grating single-mode DFB laser," *IEEE journal of quantum electronics*, vol. 28, no. 7, pp. 1653-1662, 1992.

[17] K. B. Dossou, L. C. Botten, and C. G. Poulton, "Semi-analytic impedance modeling of three-dimensional photonic and metamaterial structures," *JOSA A*, vol. 30, no. 10, pp. 2034-2047, 2013.

[18] K. B. Dossou, C. G. Poulton, and L. C. Botten, "Effective impedance modeling of metamaterial structures," *JOSA A*, vol. 33, no. 3, pp. 361-372, 2016.

[19] H. Han and J. Coleman, "Two-dimensional rectangular lattice distributed feedback lasers: A coupled-mode analysis of TE guided modes," *IEEE journal of quantum electronics*, vol. 31, no. 11, pp. 1947-1954, 1995.

[20] T. Rozzi, "Rigorous analysis of the step discontinuity in a planar dielectric waveguide," *IEEE Transactions on Microwave Theory and Techniques*, vol. 26, no. 10, pp. 738-746, 1978.

[21] P. Yeh, A. Yariv, and C.-S. Hong, "Electromagnetic propagation in periodic stratified media. I. General theory," *JOSA*, vol. 67, no. 4, pp. 423-438, 1977.

[22] D. J. Griffiths and C. A. Steinke, "Waves in locally periodic media," *American Journal of Physics*, vol. 69, no. 2, pp. 137-154, 2001.

[23] R. E. Collin, "Field theory of guided waves," 1960.

[24] A. Ghatak, K. Thyagarajan, and M. Shenoy, "Numerical analysis of planar optical waveguides using matrix approach," *Journal of lightwave technology*, vol. 5, no. 5, pp. 660-667, 1987.

[25] P. Yeh, *Optical waves in layered media*. Wiley-Interscience, 2005.

[26] C. Elachi, "Waves in active and passive periodic structures: A review," *Proceedings of the IEEE*, vol. 64, no. 12, pp. 1666-1698, 1976.

[27] P. Pereyra, "Theory of finite periodic systems: the eigenfunctions symmetries," *Annals of Physics*, vol. 378, pp. 264-279, 2017.

[28] P. Yeh, "Resonant tunneling of electromagnetic radiation in superlattice structures," *JOSA A*, vol. 2, no. 4, pp. 568-571, 1985.

[29] K. Sakai, E. Miyai, T. Sakaguchi, D. Ohnishi, T. Okano, and S. Noda, "Lasing band-edge identification for a surface-emitting photonic crystal laser," *IEEE Journal on Selected Areas in Communications*, vol. 23, no. 7, pp. 1335-1340, 2005.

[30] M. Koba and P. Szczepanski, "Coupled mode theory of photonic crystal lasers," in *Photonic Crystals-Introduction, Applications and Theory*: InTech, 2012.

[31] O. Painter *et al.*, "Two-dimensional photonic band-gap defect mode laser," *Science*, vol. 284, no. 5421, pp. 1819-1821, 1999.
[32] L. Mahler *et al.*, "Quasi-periodic distributed feedback laser," *Nature Photonics*, vol. 4, no. 3, p. 165, 2010.

7. Appendix: Derivation of Chebyshev Identity

The derivation can be found in reference [4], [20] and [21] but briefly here. According to the Floquet theorem, in an infinite periodic structure with period L, field at x and $x+L$ has no difference except a complex constant. Hence the Bloch wave satisfies the following eigenvalue problem:

$$\mathbf{m}\Psi = e^{-j\mathrm{K}L}\Psi \tag{A1}$$

where Ψ is the eigen-vector (normalized) of the matrix $\mathbf{m}$ whose eigenvalue is $\exp(-j\mathrm{K}L)$. $\mathbf{m}$ is the unit-cell translation matrix $(m_{11}, m_{12}, m_{21}, m_{22})$ and is given by equation (5).

Equation (A1) gives:

$$\det(\mathbf{m} - e^{-j\mathrm{K}L}\mathbf{I}) = 0 \tag{A2}$$

or equivalently:

$$e^{\pm j\mathrm{K}L} = \frac{1}{2}(m_{11}+m_{22}) \pm \sqrt{\frac{1}{4}(m_{11}+m_{22})^2 - 1} \tag{A3}$$

Suppose $\mathbf{m}$ is diagonalizable, chosen $\mathbf{P}$ such that

$$\mathbf{P}^{-1}\mathbf{m}\mathbf{P} = \begin{pmatrix} e^{+j\mathrm{K}L} & 0 \\ 0 & e^{-j\mathrm{K}L} \end{pmatrix} \tag{A4}$$

Then

$$\left(\mathbf{P}^{-1}\mathbf{m}\mathbf{P}\right)^N = \begin{pmatrix} e^{+jN\mathrm{K}L} & 0 \\ 0 & e^{-jN\mathrm{K}L} \end{pmatrix} = \mathbf{P}^{-1}\mathbf{m}^N\mathbf{P} \tag{A5}$$

Hence

$$\mathbf{m}^N = \begin{pmatrix} e^{+jN\mathrm{K}L} & 0 \\ 0 & e^{-jN\mathrm{K}L} \end{pmatrix} = \mathbf{P}\begin{pmatrix} e^{+jN\mathrm{K}L} & 0 \\ 0 & e^{-jN\mathrm{K}L} \end{pmatrix}\mathbf{P}^{-1} \tag{A6}$$

i.e. the Nth power of the transformed matrix is equal to the transform of the Nth power of the matrix. The matrix $\mathbf{P}$ that can transform $\mathbf{m}$ into a diagonal matrix can be constructed by the eigenvectors of $\mathbf{m}$. Hence, the equation (A6) yields:

$$\mathbf{m}^N = \begin{pmatrix} \dfrac{m_{11}\sin N\mathrm{K}L - \sin(N-1)\mathrm{K}L}{\sin \mathrm{K}L} & \dfrac{m_{12}\sin N\mathrm{K}L}{\sin \mathrm{K}L} \\ \dfrac{m_{21}\sin N\mathrm{K}L}{\sin \mathrm{K}L} & \dfrac{m_{22}\sin N\mathrm{K}L - \sin(N-1)\mathrm{K}L}{\sin \mathrm{K}L} \end{pmatrix} \tag{A7}$$

And from (A3):

$$\cos \mathrm{K}L = \frac{1}{2}(m_{11}+m_{22}) \tag{A8}$$

Hence

$$\mathrm{K}L = \cos^{-1}\left[\frac{1}{2}(m_{11}+m_{22})\right] \tag{A9}$$

In mathematics, polynomial with the form of

$$U_N = \frac{\sin(N+1)\theta}{\sin\theta}$$

is known as Chebyshev polynomials of the second kind. Hence the Nth power of the unimodular matrix is given by:

$$\mathbf{m}^N = \begin{pmatrix} m_{11}U_{N-1} - U_{N-2} & m_{12}U_{N-1} \\ m_{21}U_{N-1} & m_{22}U_{N-1} - U_{N-2} \end{pmatrix}$$